PREGALACTIC FORMATION OF GLOBULAR CLUSTERS IN COLD DARK MATTER[1]

EDWARD I. ROSENBLATT,[2] S. M. FABER, AND GEORGE R. BLUMENTHAL
Lick Observatory, Board of Studies in Astronomy and Astrophysics, University of California, Santa Cruz

ABSTRACT

We reconsider the pregalactic hypothesis for the formation of globular clusters in the light of Zinn's discovery published in 1985 of a two-component globular population in the Milky Way. For a cold dark matter spectrum, high-σ fluctuations of 10^5–10^6 $M_\odot$ are assumed to be the progenitors of the spheroidal population of globular clusters. The mass fraction of globular clusters in galaxies then requires that perturbations above rougly 2.8 σ survive as globulars, and their observed radii require baryonic collapse factors of order 10. Such an absolute density threshold for globular cluster formation achieves adequate fits to observed cluster radii and densities, the mass fraction of globulars versus Hubble type, the radial density profile of globulars within galaxies, and the globular luminosity function. However, a fixed density threshold criterion for cluster survival lacks convincing physical justification and does not by itself explain the homogeneous metallicities within clusters or the large metallicity variations from cluster to cluster and from galaxy to galaxy.

Subject headings: clusters: globular — dark matter — stars: formation

I. INTRODUCTION

The baryonic Jeans mass after decoupling in the early universe was 10^5 $M_\odot$ (Peebles and Dicke 1968). For a flat or monotonically declining density fluctuation spectrum, the first structures to collapse by gravitation would have had this minimum mass. Peebles and Dicke suggested that such structures can be identified with present-day globular clusters. Such a picture in which globular clusters form well before galaxies is often called the "primordial," or "pregalactic," model for globular cluster formation.

As theories for the shape and amplitude of the initial density fluctuation spectrum have developed, it is now possible to predict not only the masses but also the radii, densities, and collapse epochs of early collapsing objects. Peebles (1984) reconsidered the pregalactic model in the context of the cold dark matter (CDM) density fluctuation spectrum, in which perturbations on any mass scale have a Gaussian distribution. His estimated radii for collapsed protoglobular clusters were rather large: ~ 1 kpc for a 3 σ perturbation of 10^8 $M_\odot$. If true, this would argue against pregalactic fluctuations since observed globular radii are much smaller, by a factor of about 100. Very large baryonic collapse factors would be required, inconsistent with reasonable limits on initial angular momenta (Peebles 1980).

A second class of models has globulars forming somewhat later, during the galaxy collapse process itself. Such models might be termed "secondary" models. Examples include the suggestion by Fall and Rees (1985) that globulars formed from a two-phase thermal instability in 10^6 K protogalactic gas, or Gunn's (1980) cloud-cloud collision model involving shock-induced cooling.

In yet a third class of models, which we designate as "tertiary," globulars continue to form well after active collapse has ceased and perhaps even throughout the lifetime of a galaxy. This category would also include any clusters that might have formed via galaxy-galaxy interactions.

Observations of globulars themselves suggest they may constitute an inhomogeneous population that formed in a variety of ways (Burstein 1987). Young and intermediate-age "populous" clusters that are morphologically similar to globulars are frequent in the Magellanic Clouds (e.g., Freeman 1980) and in M33 (Christian and Schommer 1983). NGC 2158 is a rich, middle-aged cluster far from the Sun near the plane of the Milky Way. For years it was classified as a true globular based on morphology and richness, but its turnoff age is only 3×10^9 yr (Christian, Heasley, and Janes 1985). Intermediate-age globulars may also exist in M31 and M33 (Burstein et al. 1984).

An important recent study of Milky Way globulars by Zinn (1985) addresses the question of their homogeneity. Zinn concludes on both spatial and dynamical grounds that Milky Way globulars divide naturally into two groups: a "halo" population spherically distributed throughout the halo with low rotation and low metals, and a "disk" population concentrated toward the Galactic center with a highly flattened spatial distribution, high rotation, and relatively high metals. Individual globulars can be assigned to the two groups on the basis of composition—Zinn puts the dividing line at [Fe/H] $= -0.8$. An important by-product of this new picture is the fact that there is little or no evidence for any metallicity gradient within the halo population itself. The apparent abundance gradient within the cluster system is due instead to the changing ratios of the disk and halo populations versus radius. A further implication is that only the halo population should properly be compared to either pregalactic or secondary models of cluster systems. The disk system apparently formed after the gas collapsed to a rotating disk and is thus a tertiary component.

Zinn's proposal has led us to a new consideration of the pregalactic model. We have always considered a serious weakness of this model to be its difficulty in explaining the radial abundance gradient of globulars within the Galaxy. This weakness stems from the fact that pregalactic globulars by definition form well in advance of galaxy collapse. There is thus no natural mechanism whereby metallicity ought to correlate with final position. In an effort to address this question, Peebles

(1984) speculated that, owing to statistical correlations with environment, inner globulars would be denser and more able to retain metals produced by their own supernovae. Although inner clusters are indeed denser in the CDM picture (see below), the metallicity distribution within individual globulars is not broad enough to suggest much self-enrichment. All self-enriched models with constant IMF (with or without gas loss) predict an internal spread in [Fe/H] of at least 0.5 dex (e.g., Zinn 1978), whereas a spread of this magnitude is seen only in ω Cen and possibly in M22 (Kraft 1979). Zinn's identification of a *gradient-free* halo population solves the problem nicely by removing any need for such a correlation.

In this paper we reevaluate the pregalactic model in the context of cold dark matter by making a more detailed comparison with the observed structural properties of halo globular clusters. We stress a point implicit in Peebles's picture, but not much emphasized by him, that the most natural identification with globulars is achieved using high-σ, strongly overdense perturbations. High overdensity lessens the required baryonic collapse factors and generally improves the match with observations. It is also implicit in this model that each globular is surrounded initially by a dark matter halo. However, most of the mass is outside the visible structure and does not affect the observable cluster dynamics. The halo is also probably tidally stripped during galactic collapse, and the dark matter left today is substantially reduced from its initial value.

A major uncertainty is whether the structural parameters of globulars today reflect their primordial values. There are a number of processes that may have altered those parameters over the years, including tidal stripping, mass loss, and two-body relaxation. For the most part we have ignored these effects because of their complexity, but the models have a degree of uncertainty on that account.

A second major question is how to decide which fluctuations survive as globular clusters as opposed to those that are destroyed in the collapse of higher mass fluctuations. We consider three possible models, and for one of these, which we call the fixed-density model, we obtain a fair match to globular radii, densities, mass fraction versus Hubble type, and luminosity function. However, this particular scheme is not well motivated physically, and there still remain significant puzzles surrounding the origin of globular cluster metallicities. In the end, we conclude that the adequacy of the pregalactic model, even for halo globular clusters, remains somewhat problematic.

As stated previously, we do not believe the pregalactic model is necessarily the only mechanism whereby globulars can form. Observations of globular clusters in our Galaxy and others suggest that the true picture is more complicated. We examine the pregalactic model keeping in mind that any single cluster system may represent a population of objects formed from several processes, including pregalactic, secondary, and tertiary phases. Several of our conclusions about the pregalactic model were noted, but more briefly, in a recent review by Fall and Rees (1986).

II. COMPARISON WITH OBSERVED CLUSTER PROPERTIES

a) Globular Mass Fractions in Galaxies

The calculations in this paper make use of the cold dark matter spectrum computed by Primack and Blumenthal (1985) and discussed in the context of galaxy formation by

Blumenthal et al. (1984, hereafter BFPR). As noted previously, a key assumption of the pregalactic model is exactly which density perturbations at a given mass survive as globular clusters. Let us assume for the moment that all $10^6 M_\odot$ perturbations everywhere in the universe above some $n\sigma$ survive as globulars. Such a trend is plausible since dense perturbations have at least two survival advantages over their low-density counterparts. They collapse at an earlier epoch relative to their parent galaxy and are therefore not as easily disrupted by parent galaxy collapse. In addition, their higher binding energy may allow them to survive better against cluster-cluster tidal collisions and supernovae explosions. Relative to 1 σ fluctuations at a given mass, the equilibrium radii of collapsed $n\sigma$ fluctuations scale as n^{-1}, their collision cross section as n^{-2}, their collapse times as $n^{-3/2}$, and their densities as n^{-3}.

With CDM the density distribution function is Gaussian, and the fraction of mass in perturbations above 2 σ is 2.3%, and above 3 σ is 0.13%. These values are compared to observed globular mass fractions in galaxies in Figure 1. Details are given in the legend and Table 1. Baryon masses of globulars and galaxies are based on their observed luminosities plus mass-to-light ratios from stellar population models. From the figure, cluster mass fractions average around 0.25%, implying $n = 2.8$. This value is only a lower limit if contamination by tertiary clusters is important. We believe that such contamination may be severe in dwarf galaxies and may account for their somewhat high mass fractions in Figure 1. Tertiary contamination in large galaxies is probably not a significant factor, however. For example, if the tertiary fraction in our Galaxy based on Zinn's (1985) counts is typical of spirals generally, the median spiral mass fraction would decrease to 0.17%, and

TABLE 1
GLOBULAR CLUSTER–GALAXY MASS FRACTION DATA

Object	Type	M_V[a,b]	N_{obs}[b]	N_t[b]	$100 M_{cl}/M_g$	$\log M_{cl}/M_g$
M31	S	−21.1	300	450	0.16	−2.80
Galaxy	S	−20.0	131	180	0.18	−2.74
LMC	I	−18.5	17	23	0.30	−2.52
SMC	I	−16.8	10	15	0.85	−2.07
M33	S	−18.9	6	20	0.06	−3.22
Fornax	dSph	−13.6	6	6	3.3	−1.48
NGC 147	dE	−14.9	4	4	0.65	−2.19
NGC 185	dE	−15.2	6	7	0.90	−2.05
NGC 205	dE	−16.4	8	8	0.33	−2.48
NGC 6822	I	−15.7	0	0	<0.16[c]	< −2.80[c]
IC 1613	I	−14.8	0	0	<0.35[c]	< −2.46[c]
WLM	I	−16.0	1	1	0.12	−2.92
NGC 4216	S	−21.0	21	520	0.20	−2.70
NGC 4340	E	−19.9	26	650	0.35	−2.46
NGC 4374	E	−21.6	98	2500	0.28	−2.55
NGC 4406	E	−21.7	108	2600	0.26	−2.59
NGC 4472	E	−22.5	1700	4200	0.20	−2.70
NGC 4486	E	−22.3	6000	15000	0.88	−2.06
NGC 4526	E	−21.3	87	2200	0.32	−2.49
NGC 4564	E	−20.0	35	900	0.44	−2.36
NGC 4569	S	−21.4	32	800	0.22	−2.66
NGC 4594	S	−22.6	290	2800	0.25	−2.60
NGC 4596	E	−20.4	82	2000	0.67	−2.17
NGC 4621	E	−21.1	63	1600	0.28	−2.55
NGC 4636	E	−21.3	143	3600	0.53	−2.28
NGC 4649	E	−22.1	170	4200	0.30	−2.52
NGC 4697	E	−21.6	72	1800	0.20	−2.70

[a] $H_0 = 75$ km s^{-1} Mpc^{-1} is assumed.
[b] From Harris and Racine 1979.
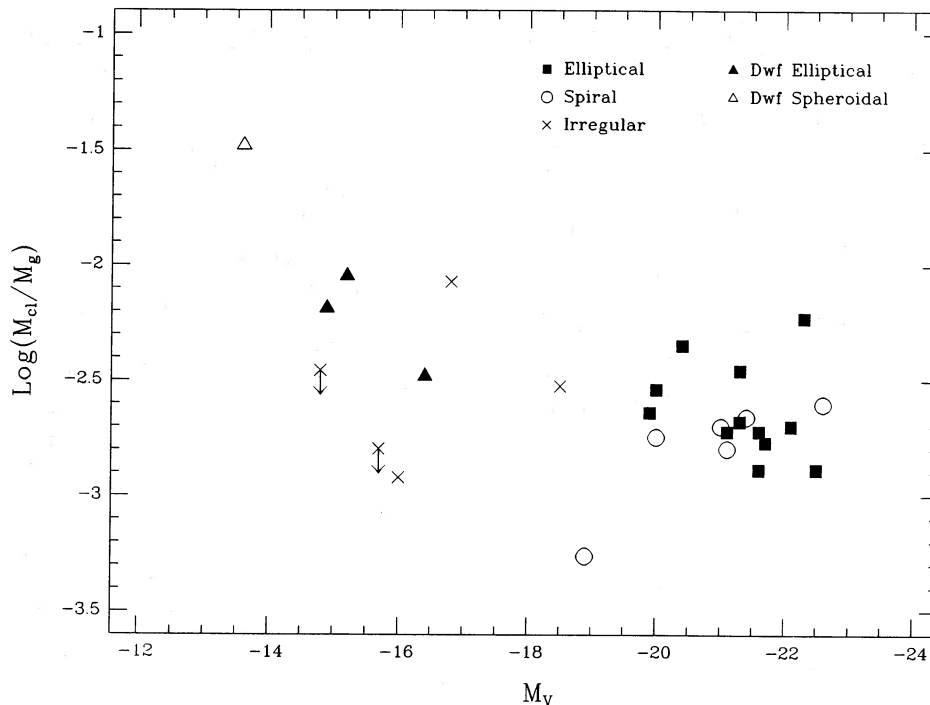[c] Upper limit assumes one globular cluster of $2.5 \times 10^5 M_\odot$ (baryonic) in the galaxy.

FIG. 1.—Globular cluster mass fraction, M_{cl}/M_g, vs. galaxy absolute magnitude from the data of Harris and Racine (1979). Total baryon mass in clusters is taken to be $N_t m_{cl}$, where m_{cl}, the mean individual cluster mass, is $2.5 \times 10^5 \, M_\odot$, corresponding to the average luminosity of a Milky Way cluster and $M/L_V = 1.6$ (Illingworth 1976). N_t is the estimated total number of globulars in each galaxy from Harris and Racine, with typical estimated errors of perhaps a factor of 2 or greater. Galaxy baryon mass is derived from Harris and Racine's absolute V magnitudes, plus assumed baryonic M/L_V as follows: E = 6; Spirals = 3; Dw E and Dw Sph = 2; Irr = 1. Cluster-to-galaxy total mass ratios are assumed to equal the baryon ratios. For massive galaxies the median value of M_{cl}/M_g is $\sim 0.25\%$, implying cluster formation for perturbations above 2.8 σ.

hence $n = 2.9$, only slightly larger. Our conclusion is that values of $n \approx 3$ are required by the model, which in view of the above scaling relations, might be high enough to give over-dense protoclusters a plausible survival edge.

b) Three Survival Scenarios

It is desirable to have a more precisely defined survival criterion. We therefore consider three possible subscenarios.

In the first scenario, called the *fixed-density* model, the amplitude of a peak is defined globally. Therefore, peaks at a given σ level all correspond to the same specific density at all points in the universe. The flatness of the CDM spectrum implies that there are substantial statistical correlations between peaks on different mass scales (Peebles 1984; BFPR; Bardeen *et al.* 1986; Peacock and Heavens 1986). Therefore, fixed-density peaks above, say, 2.8 σ, will be relatively more common in overdense parent galaxies and hence will be as common there as lower σ peaks elsewhere. The magnitude of this effect is calculated in § IIc below.

In the second scenario, called the *fixed-probability* model, the likelihood of finding a peak is defined locally, i.e., one considers the probability of finding a peak within a specific larger region. In this case, the σ of a peak is only a measure of its *local* probability, and 2.8 σ peaks would be equally common in both overdense and underdense larger regions, but they would correspond to higher densities in overdense regions. Such peaks turn up with equal frequencies everywhere. Depending on the context, the size of the larger region can range from a galactic mass down to 10^{-2} to 10^{-3} times a galactic mass, the latter case corresponding to a localized environment within a protogalaxy.

Neither of the above scenarios is strongly motivated by physics, as neither takes into account the detailed interactions between protoglobulars and the density perturbations in which they are embedded. We attempt to do this by considering yet a third model, in which survival depends on the existence of a minimum density contrast between the protoglobular and its environment. For simplicity we generally consider just density contrast against the parent galaxy. This alternative will be called the *density-contrast* model.

Unfortunately, all of these three models are highly schematic. To do better, however, would require numerical simulations for cluster survival on a scale that is beyond our present capabilities.

c) Radii and Densities of Globulars in the CDM Scenario: Dependence on Hubble Type and Spheroid Mass

We first compare the expected structural properties of clusters in the three scenarios with those of clusters in the Milky Way. The approach used is identical to that of BFPR, who compared galaxies and clusters of galaxies with higher mass fluctuations. Comparisons are rough, being based on a simple spherical top-hat model for collapsing perturbations. Within that framework, however, we have made an attempt to arrive at consistent definitions of mass, potential energy, kinetic energy, radius, virial temperature, and baryon density to compare with observations (see Table 2). Further details are given in Figure 3 of BFPR and the figure legend here.

Figures 2a, 2b, and 2c illustrate the results. The solid lines represent the fixed-density model and show the equilibria of collapsed 1 σ, 2 σ and 3 σ perturbations sampled over the whole universe. These loci refer to objects that collapse dissi-

TABLE 2
DATA ON 65 GALACTIC GLOBULAR CLUSTERS

NGC	$\log n_b$	$\log T$	[Fe/H][a]	r(GC)[b]	R_V[c]	$10^{-5}M_c$[d]	v(km s^{-1})[e]
104...	3.9	3.92	−0.71	6.4	10	8.0	18.57[f]
362...	4.0	3.65	−1.27	8.1	6.8	2.9	13.53[f]
1261...	3.5	3.21	−1.29	15.5	7.1	1.1	8.19
1851...	4.6	3.69	−1.33	14.4	3.6	1.7	14.18[f]
1904...	3.4	3.27	−1.68	17.0	8.4	1.5	8.80
2419...	1.3	3.12	−2.10	95.8	70	8.8	7.36
2808...	4.6	4.09	−1.37	9.7	5.5	6.4	22.46
3201...	3.0	3.07	−1.56	7.8	11	1.2	6.91
4590...	3.7	3.18	−2.09	9.2	5.2	0.72	7.85
4833...	3.6	3.27	−1.86	6.1	7.1	1.4	8.73
5024...	2.8	3.35	−2.04	18.2	17	3.7	9.65
5053...	1.4	2.23	−2.58	17.0	25	0.40	2.60
5139...	3.3	3.94	−1.59	5.6	20	17	18.98
5272...	2.0	3.22	−1.66	10.6	38	6.0	8.31[g]
5466...	1.5	2.43	−2.22	15.6	29	0.74	3.34
5694...	3.5	3.20	−1.92	24.9	7.8	1.4	8.04
5824...	3.9	3.64	−1.87	17.9	6.8	2.9	13.46
5897...	2.6	2.85	−1.68	6.8	13	0.86	5.39
5904...	3.2	3.52	−1.40	5.5	13	4.2	11.76
5986...	2.9	3.41	−1.67	4.2	17	4.3	10.34
6093...	4.4	3.71	−1.68	2.9	4.5	2.2	14.58
6121...	3.7	3.16	−1.28	5.4	5.2	0.69	7.66
6144...	2.8	2.78	−1.75	2.9	9.7	0.56	4.99
6171...	0.68	2.83	−0.99	3.0	115	7.5	5.28
6205...	3.1	3.42	−1.65	7.5	14	3.4	10.43
6218...	2.6	3.03	−1.61	3.7	16	1.6	6.63
6229...	2.9	3.22	−1.54	27.6	14	2.2	8.23
6254...	3.7	3.32	−1.60	4.0	6.5	1.3	9.28
6266...	3.9	3.75	−1.29	2.3	8.1	4.3	15.21
6273...	2.4	3.36	−1.68	3.4	28	6.2	9.73
6284...	4.6	3.48	−1.24	3.5	2.6	0.78	11.24
6287...	3.9	3.19	−2.05	1.6	4.2	0.61	7.98
6293...	3.9	3.32	−1.92	1.0	5.2	1.0	9.34
6304...	4.0	3.32	−0.59	2.7	4.5	0.90	9.30
6333...	4.2	3.47	−1.78	1.5	4.2	1.2	10.98
6341...	4.1	3.61	−2.24	8.7	5.5	2.1	12.97
6352...	4.0	3.14	−0.51	3.3	3.6	0.45	7.55
6356...	3.9	3.70	−0.62	6.8	7.8	3.8	14.46
6362...	3.4	2.94	−1.08	4.4	5.5	0.46	5.98
6397...	3.3	2.98	−1.91	5.5	6.8	0.61	6.22
6402...	3.2	3.67	−1.39	3.9	16	7.2	13.82
6426...	1.4	2.20	−2.20	10.7	24	0.37	2.56
6522...	4.7	3.55	−1.44	1.0	2.6	0.86	12.09
6528...	4.5	3.43	0.12	2.0	2.9	0.75	10.55
6541...	4.0	3.57	−1.83	2.0	5.8	2.1	12.37
6553...	3.8	3.53	−0.29	2.7	7.5	2.4	11.83
6626...	4.2	3.65	−1.44	2.3	5.2	2.2	13.56
6637...	3.8	3.46	−0.59	1.5	6.8	1.9	10.95
6638...	4.3	3.29	−1.15	1.3	2.9	0.53	8.94
6656...	4.1	3.72	−1.75	4.1	6.5	3.2	14.65
6712...	3.4	3.20	−1.01	3.3	7.5	1.1	8.09
6715...	3.8	3.87	−1.43	12.0	11	7.7	17.55
6723...	3.3	3.20	−1.09	2.4	8.4	1.3	8.14
6752...	3.8	3.46	−1.54	4.5	6.2	1.7	10.86
6760...	4.5	3.42	−0.52	4.7	2.7	0.69	10.44
6779...	3.1	3.11	−1.94	8.7	9.7	1.2	7.28
6809...	3.5	3.10	−1.82	3.3	6.2	0.72	7.21
6838...	3.2	2.66	−0.58	5.9	5.2	0.23	4.36
6864...	4.5	3.81	−1.32	10.5	4.5	2.8	16.28
6934...	3.8	3.32	−1.54	10.1	5.5	1.1	9.27
6981...	2.7	2.85	−1.54	11.4	12	0.79	5.39
7006...	2.7	2.99	−1.59	33.0	14	1.3	6.32
7078...	4.2	3.88	−2.15	9.5	6.5	4.8	17.75
7089...	3.9	3.78	−1.62	9.6	8.7	5.0	15.84
7099...	4.3	3.42	−2.13	6.5	3.6	0.91	10.39

[a] From Zinn 1985.
[b] r(GC) is the distance from the galactic center in kpc.
[c] $R_V = GM_c/v^2$ is given in parsecs.
[d] Cluster mass, M_c, in units of $10^5\ M_\odot$. M_c is taken to be $M_c = 1.6L_c$, where L_c is the observed cluster luminosity from Harris and Racine 1979.
[e] $v^2 = 3\sigma^2$, where σ is taken from Peterson and King 1975 or as noted.
[f] Illingworth 1976.
[g] Gunn and Griffin 1979.

pationlessly, their density represented by the baryonic component ($n_b = 0.1n_{tot}$). The contraction track in Figure 2a schematically illustrates baryon evolution under radiative dissipation within dark halos. The black dots are globular clusters in the Milky Way halo population, to be compared with the pregalactic model; open circles represent disk clusters, which are included for comparison.

The vertical density displacement between the observed globulars and the models in Figure 2 is a measure of the required radial baryonic collapse factor ($r \approx n_b^{-1/3}$). Comparison with the 3 σ curve shows that radial collapse factors of order 10 are needed, substantially reduced from the factor of 100 in Peebles' original estimate. This is due, we believe, to the attempt here to define all structural quantities self-consistently. Radial collapse factors of this magnitude are still difficult to account for physically, especially when the collapsed remnants rotate as slowly as globular clusters. However, elliptical galaxies may have collapsed by a comparable factor yet also rotate slowly. Perhaps a similar mechanism acts to reduce rotation in both cases. If this objection can be tolerated, we conclude that the fixed-density model offers a reasonable fit to the radii and densities of observed clusters.

As depicted in Figure 2, Milky Way globulars exhibit a fairly large spread in baryonic density at a given virial temperature. This spread may result from varying degrees of dissipation or may reflect observational errors (mass is probably better determined from the present data than either density or velocity dispersion). A third possibility is cluster formation from perturbations over a range of initial $n\sigma$.

Next we estimate the radii and densities of globulars in the fixed-probability model. To do so, it is necessary to understand how protoglobular perturbations would depend on parent galaxy overdensity in the CDM picture. The methods for calculating such correlations have been developed by Peebles (1984), Bardeen et al. (1986), Peacock and Heavens (1986), and G. R. Blumenthal (unpublished). They are used here to calculate how the distribution of density fluctuations on a small mass scale, M_1, correlates with overdensity on a parent mass scale, M_2, where the two masses are assumed to be spherical and concentric. The results for $M_1 = 10^6\ M_\odot$ and $M_2 = 10^{12}\ M_\odot$ are illustrated in Figure 3, where the Gaussian dashed curve shows the distribution of $10^6\ M_\odot$ fluctuations for the whole universe with rms width taken to be unity. This is superposed on four solid curves that correspond to M_1 fluctuations embedded within $10^{12}\ M_\odot$ perturbations of various degrees of overdensity, as indicated. The embedded distributions exhibit a mean offset that is proportional to parent overdensity and an rms Gaussian width that is slightly narrower than the distribution for the universe as a whole. Additional calculations (not shown) indicate that the probability distributions in Figure 3 vary only slowly with radius for $R < R_{TH}$ inside a top-hat fluctuation.

Similar correlations have been calculated for other values of M_1 and the results translated into the densities and temperatures of collapsed objects in the n_b, T plane in Figures 2a, 2b, and 2c (dashed lines). The σ's labeling the curves are now locally defined within a galaxy and are measured in units of the rms widths of the embedded distributions in Figure 3. These dashed curves are the predictions of the fixed-probability model.

Figures 2a, 2b, 2c show that 1 σ fluctuations within a 3 σ parent are considerably denser than the average 1 σ fluctuations, whereas 2 σ and 3 σ fluctuations remain more similar. This is so because the positive enhancement due to the mean offset is effectively canceled by the narrower σ, leaving 2 σ and
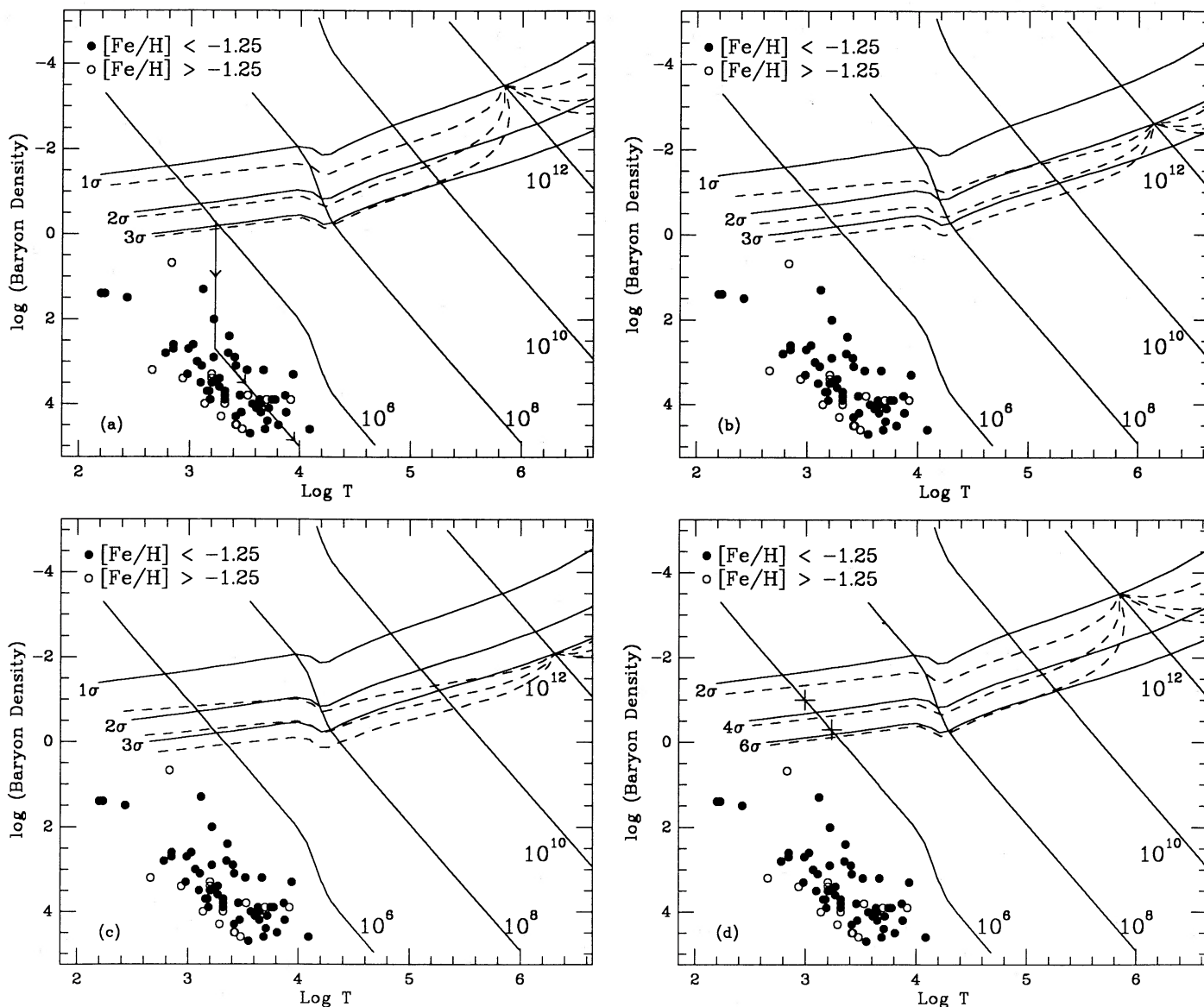
Fig. 2.—(a) Baryonic density vs virial temperature for theoretical collapsed objects and Galactic globular clusters. The precepts used to define n_b and T are identical to those in Fig. 3 of BFPR. The dots represent Galactic halo globular clusters; the open circles are disk globulars shown for comparison. Velocity dispersions for Galactic globulars come from theoretical estimates by Peterson and King (1975) for $M/L_V = 1.6$ (Illingworth 1976); some directly observed values are also used (Illingworth 1976; Gunn and Griffin 1979). Globular masses are estimated from Harris and Racine's M_V's and $M/L_V = 1.6$. From these we deduce a virial radius $R_V \equiv GM/3\sigma^2$, and baryonic density $n_b \equiv 3M/4\pi R_V^3$. For further details see Table 2. Solid curves represent collapse loci for dissipationless collapse of 1 σ, 2 σ, and 3 σ perturbations from a cold dark matter density fluctuation spectrum, with n_b assumed to be $0.1 n_{\rm tot}$. The diagonal lines show the total mass of a perturbation including dark matter. The track leading downward through the clusters is a schematic dissipation track. For an assumed total cluster mass of $10^6 M_\odot$ and an initial overdensity of 2.8 σ (§ IIa), this track agrees fairly well with the observed properties of clusters. The dashed curves show how the collapse loci change if perturbations are embedded within a $10^{12} M_\odot$ fluctuation of 1 σ overdensity. Both embedded and parent perturbations are assumed to be concentric and spherical. Embedded perturbations of 1 σ are significantly more overdense than average, but 2 σ and 3 σ perturbations are only slightly altered. See text for further details. (b) Same as (a) except that the dashed lines refer to a 2 σ fluctuation of $10^{12} M_\odot$. (c) Same as (a), except that the dashed line refer to a 3 σ fluctuation of $10^{12} M_\odot$. (d) Similar to (a) except that the effect of biased galaxy formation is included. Spirals are assumed to be 2 σ fluctuations instead of 1 σ, as above. All curves scale likewise, now referring to 2 σ, 4 σ, and 6 σ perturbations (solid lines) embedded within a 2 σ galaxy (dashed lines). The location of $10^6 M_\odot$ fluctuations at 5.6 σ and 2.8 σ are indicated by the two crosses.

3 σ fluctuations at about the average levels. Figure 3 implies that this near constancy begins to break down in parent fluctuations below 1 σ, where offset and σ no longer balance. The effect becomes stronger in negative-density fluctuations, where high-density $10^6 M_\odot$ peaks are predicted to be quite rare. The main point is that the predissipation radii and density of clusters in the fixed-probability model would not differ much from the fixed-density case, as indicated by the fact that the solid

and dashed 2 σ and 3 σ curves in Figures 2a, 2b, and 2c are substantially the same. Therefore it is likely that the final properties after dissipation would also be the same.

Finally, we consider the density-contrast model, in which survival requires a minimum density contrast between a globular cluster and the parent galaxy. Since high-σ parents are smaller and denser (see Fig. 2), protoglobular perturbations within them must be smaller and denser to survive. For
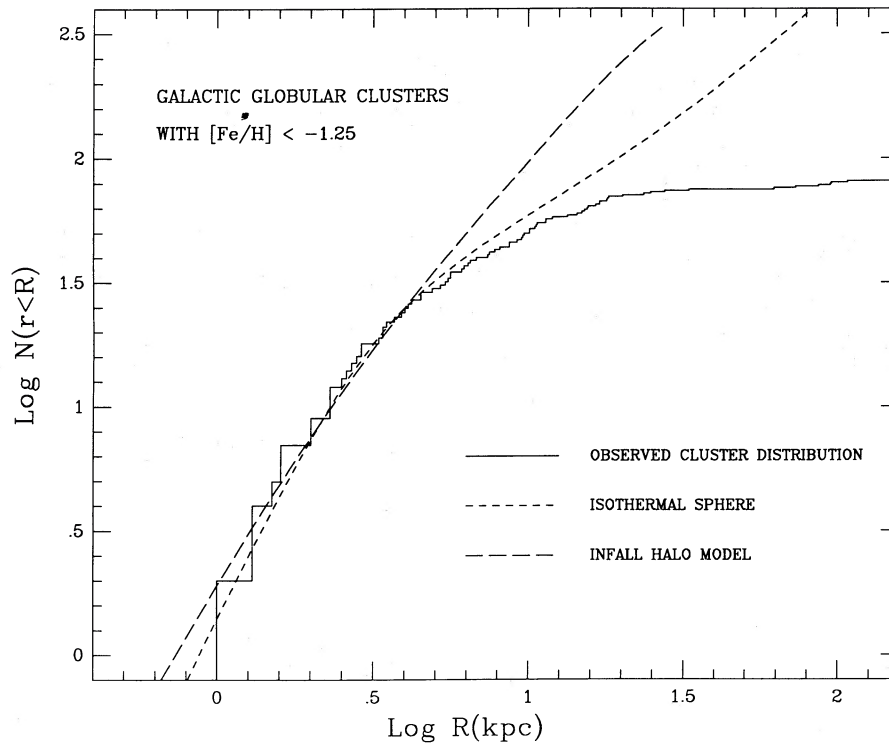
FIG. 3.—Distribution functions for the quantity $\delta \equiv \delta M/M$ for $10^6 M_\odot$ spherical volumes in a CDM universe. The dashed curve refers to the universe as a whole, and the horizontal axis is in units of this global σ. The solid curves show the conditional distribution of δ for concentric spheres embedded within $10^{12} M_\odot$ spherical fluctuations of overdensity, σ_p, as shown. There is a mean offset in δ that is proportional to parent galaxy overdensity, and the σ of the conditional distribution is reduced.

example, if the contrast threshold is assumed to be fixed, in a 3 σ parent, protoglobulars would have to be smaller by a factor of 3 and denser by a factor of 27. This strong dependence on the nature of the parent is not predicted in the other two cases.

Comparision of all three models with observations is possible provided one is willing to adopt a theory for the origin of galaxy Hubble types under CDM—for example, that suggested by BFPR. These authors hypothesized that Hubble type is monotonically related to overdensity such that spirals, S0's, and Es arise from 1 σ, 2 σ, and 3 σ fluctuations respectively. Actual globulars seems to show little evidence for any variation in properties with Hubble type (Harris 1987) although the data are skimpy. This lack of any correlation with Hubble type is consistent with either the fixed-density or fixed-probability models but not the density-contrast model.

Figure 2 can also be used to predict whether and how the mass fraction of globulars should vary with Hubble type. In the fixed-probability scenario, the number of surviving globulars by hypothesis is a constant fraction by mass in all regions, and there is thus no predicted dependence of globular mass fraction on Hubble type. In this model, globulars should be found with equal probability in galaxies, in intergalactic space, and even in voids if there is any matter there today. In the fixed-density model, there is a strong trend with ambient density in the sense that protoglobulars should be more frequent in early-type (high-σ) galaxies. For example, Figure 2c suggests that 2.8 σ peaks reduce to 2 σ locally in the centers of Es and would thus be nearly 9 times more frequent there. Conversely, globulars in low-density regions outside galaxies would be exceedingly rare. Finally, the density-contrast model predicts fewer globulars in early-type galaxies, as Figure 3

shows that the density contrast between globular and parent galaxy is lowest in those regions, and survival there would be correspondingly impaired. Survival would actually be *enhanced* in intergalactic space in this model.

Counts of globulars versus Hubble type are not extensive, but those that exist show substantially more globulars in early-type galaxies. The data as of 1979 are presented in Figure 1 and have been summarized more recently by van den Bergh and Harris (1982). These authors conclude that the specific frequency of globulars is 5–10 times larger in Es than in spirals and is lowest in spirals with little or no spheroid. These numbers are calculated relative to total galaxy light; the number relative to spheroid luminosity alone is more constant. This strong preference for early-type galaxies clearly favors the fixed-density model.

A final point concerns the effect of biased galaxy formation. If the average spiral comes from a 2 σ rather than a 1 σ fluctuation as assumed above, the CDM spectrum must be renormalized as in Figure 2d to maintain consistency with the amplitude of the galaxy-galaxy correlation function at $5h^{-1}$ Mpc (Davis and Peebles 1983). The previous 1 σ curve becomes 2 σ, 2 σ becomes 4 σ, and so on. Likewise, the σ levels of embedded perturbations also scale by a factor of 2. To preserve baryonic collapse factors precisely equal to those stated previously would now require clusters to originate from higher σ perturbations, so high that globular clusters would be essentially nonexistent (see lower cross in Fig. 2d). Alternatively, if clusters still arise from 2.8 σ perturbations, which preserves the observed mass fraction (*upper cross*), the required baryonic collapse factors double to roughly 20, and the low rotations of globulars become more difficult to explain. It should be

remembered that structural parameters are known only for Milky Way globulars and that globulars in other galaxies might lie higher or lower in Figure 2. Nevertheless, it appears that the low rotation of globulars would be somewhat more difficult to account for with biased CDM.

d) Radial Distribution within Galaxies

A third comparison involves the radial distribution of globular clusters within galaxies compared to the dark matter and to spheroid field stars. If globulars are completely pregalactic, they would have collapsed dissipationlessly during galaxy formation along with the dark matter. Any difference between the two distributions today must therefore reflect a difference in the initial distributions prior to collapse. In certain scenarios such a difference is expected on theoretical grounds. As noted above, with a flat spectrum as in cold dark matter, high-σ peaks are expected to be statistically less common in the outer parts of protogalaxies (Bardeen et al. 1986). Depending on exactly how protoclusters survive, the final distribution of primordial clusters could be somewhat more (or less) centrally concentrated than the dark matter distribution.

The magnitude of the effect can be estimated using the statistical methods referred to earlier. For the fixed-density model, Figure 2 shows that 2.8 σ reduces to 2.6 σ at the center of a 1 σ parent and to 2.3 σ within a 2 σ parent. The latter value would be typical for a spiral galaxy like the Milky Way, assuming biased galaxy formation. These reductions in turn imply that protoglobular perturbations would be 1.9 and 3.9 times more frequent respectively in the centers of the two types of parent galaxies. The radial density profile of the cluster system and

that of the dark halo should thus diverge by roughly the same factor over the distance from the centers to the edges of the galaxies.

For the fixed-probability case, the number density of protoglobulars by hypothesis is the same everywhere, and the cluster and dark-matter profiles should agree at all radii. Finally, the density-contrast model predicts more surviving protoglobular perturbations at the edges of galaxies, and the cluster profile should be shallower than that of the dark matter.

A crude comparison of the two density profiles for our Galaxy is shown in Figure 4. We have slightly modified Zinn's (1985) halo cluster sample to reduce contamination by disk clusters by moving his dividing line from [Fe/H] = −0.8 to −1.25. To reduce noise, we show the cumulative radial distribution for the revised halo sample (solid line). This is compared to two models for the dark matter: a traditional isothermal sphere (short dashes) and a halo infall model of Blumenthal et al. (1986) that takes into account dark matter compression by baryonic infall (long dashes; see legend for details). The models and the cluster data have been normalized at a radial distance of a few kpc.

Relative to the isothermal sphere, the halo infall model is more centrally concentrated (i.e., has a steeper slope), but both models fit the inner part of the cluster distribution adequately within the errors. However, beyond $R \approx 10$ kpc the observed clusters fall well below both models, indicating a significant paucity of clusters relative to dark matter in the outer parts of the Milky Way. A radius of 25–20 kpc is a reasonable minimum radius to assume for the dark matter halo, and by that point the divergence amounts to about a factor of 4. Since
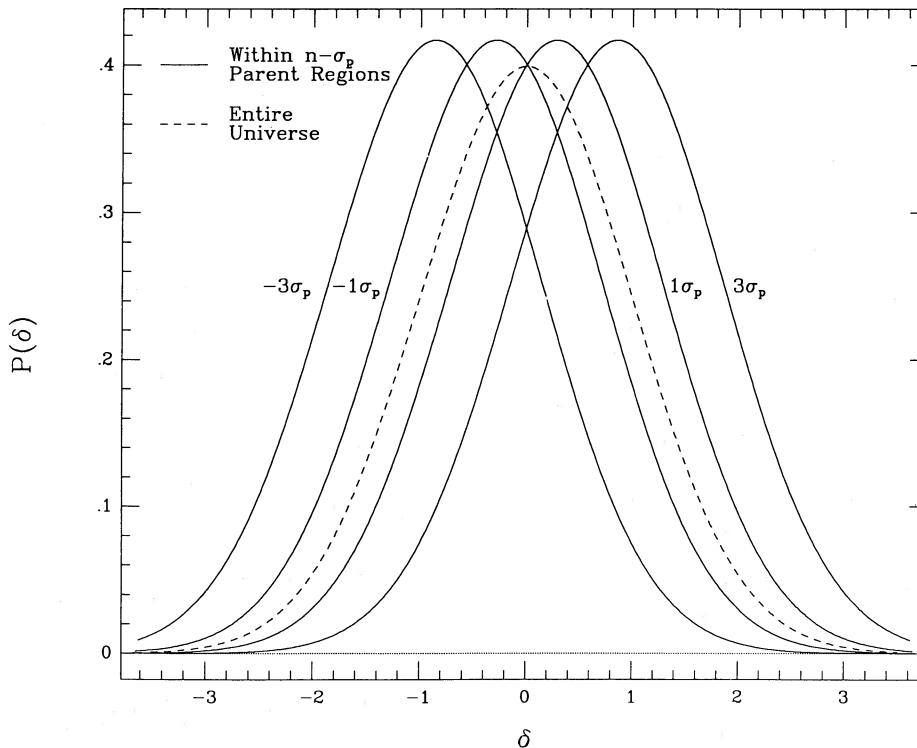

FIG. 4.—The cumulative radial distribution of Zinn's halo clusters in the Galaxy compared to two models for the dark matter. Zinn's halo sample has been trimmed at [Fe/H] = −1.25 to eliminate a few possible disk clusters. The two DM models are the standard isothermal sphere (short dashes) and a model showing the effect of baryonic infall on the DM distribution (Blumenthal et al. 1986). Relative to either DM distribution, there is a distinct paucity of observed globular clusters in the outer part of the Galaxy.

these are cumulative curves, the divergence in the space density profiles is somewhat larger still.

Once again, only the fixed-density model correctly predicts the steeper fall-off of the globular clusters. Furthermore, the model fits quantitatively only if the Milky Way is a 2 σ or so fluctuation, and hence the data are somewhat more consistent with biased galaxy formation, in contrast with the argument above concerning low cluster rotations.

Since the spheroid stars are almost certainly a highly dissipative system, all three models would suggest that primordial clusters should be significantly less concentrated relative to them. On balace this prediction is consistent with present evidence. Data on the Milky Way spheroid stars are too poor to use, but radial distributions in several ellipticals (Harris and Racine 1979; Harris and van den Bergh 1982; Forte, Strom, and Strom 1981; Lauer and Kormendy 1987) indicate that the clusters are on average less concentrated than the spheroid light, in some cases markedly so. The interpretation is still somewhat uncertain owing to possible dynamical friction and other effects which could preferentially destroy clusters in the inner regions of galaxies. However, Harris (1986) concludes that these effects are generally small over most of the radial profiles.

e) Globular Cluster Luminosity Function

A final comparison can be made with the observed luminosity function of globulars in the Local Group and Virgo cluster. This function is roughly Gaussian in magnitudes, with $\langle M_V \rangle = -7.3$ and $\sigma = 1.2$ mag (Harris and Racine 1979). For $M_V/L = 1.6$ (Illingworth 1976), this corresponds to a logarithmic mean baryonic mass of $\sim 10^5 \, M_\odot$ and a total initial mass of $\sim 10^6 \, M_\odot$ before any tidal stripping.

The existence of the lower mass cutoff at $10^{5-6} \, M_\odot$ can naturally be explained as the Jeans mass (Peebles and Dicke 1968), or alternatively as the threshold mass for efficient baryon dissipation and cooling (BFPR). The mass cutoff on the upper end, however, requires a separate explanation. To the extent that hierarchical clustering in this mass range is basically a self-similar process, it alone cannot preferentially select any particular mass value. However, since the number of globulars left behind today depends critically on survival, it seems to be possible to couple this idea with hierarchical clustering in order to provide a natural decline at higher masses. The cluster mass fractions in Figure 1 suggest that roughly 0.25% of all low-mass perturbations survive as globulars. In purely self-similar clustering, this percentage would remain constant at each level of the clustering hierarchy. Since at each level of the hierarchy the number of objects of a given mass, $dN(M)/d \log M$, scales as M^{-1}, we expect the number of surviving objects to scale likewise. Recalling that $M \propto L_V$ for constant M/L, and that $\Phi(M_V) \equiv dN(M_V)/dM_V$, we have

$$\Phi(M_V) = \text{const} \, \frac{dN(M)}{d \log M} \propto M^{-1} \propto L_V^{-1} \, , \qquad (1)$$

and also therefore

$$N(M) \propto L_V^{-1} \, . \qquad (2)$$

These expressions should be valid on all mass scales much less than a galaxy mass, $M \ll 10^{12} \, M_\odot$, where the clustering is nearly self-similar. Note that in deriving equations (1) and (2), we have not used the usual multiplicity function, as our hypothesis is that clusters of different masses are the densest

survivors from successive stages of the hierarchy, which is a diachronic concept. The multiplicity function is a snapshot of the mass distribution of fluctuations that exist at a given epoch and is a synchronic concept.

The above scenario for the luminosity function is compatible with either the fixed-density or fixed-probability models because, in both of them, the threshold σ for survival is constant at each mass level in the hierarchy, and the percentage of mass surviving in globulars at each stage is therefore also constant. The predicted luminosity function of the density-contrast model is not so clear, but it, too, could plausibly yield similar results.

Relations (1) and (2) are compared to observed luminosity functions in Figure 5. They are shown as the two straight lines, normalized to fit at the peaks. The data there have been generously communicated by William Harris and represent the most recent update of figures shown by Harris and Racine (1979). Open circles represent Local Group globulars, and closed circles data from Virgo giant ellipticals.

The relations fit the data fairly well within two magnitudes above the peak but predict too many clusters brighter than this level. For a total Local Group cluster population of ~ 450 globulars, relation (1) predicts 11 objects between $M_V = -9.8$ and -11.3, compared to an observed population of only five. The Poisson probability of seeing so few objects is 0.04. Since the predicted objects would have about the same density as normal globular clusters but have 10–30 times more mass, they would be easy to detect if present. The statistics for the Local Group are sparse but are supported by the Virgo sample.

One plausible explanation for the deficit of brightest globulars is the preferential effect of dynamical friction on higher mass objects, causing them to spiral into the central region of galaxies (Tremaine 1976; Quinn and Goodman 1986). Using equation (8) of Tremaine (1976), we estimate that the spiraling-in time from a distance of 10 kpc in M31 is less than a Hubble time for clusters above $2 \times 10^6 \, M_\odot$. Allowing for the fact that perhaps one-half or two-thirds of this mass might today be the inner remains of a dark halo, we find that this mass corresponds to $M_V \approx -9$ mag, which is about where the M^{-1} functions begin to depart from the data in Figure 5. If a little boost from dynamical friction is allowed, we conclude that, broadly speaking, any of the three survival models is able to produce a luminosity function with an upper cutoff like that observed.

III. DISCUSSION

The results of the preceding comparisons are summarized in the form of a truth table in Table 3. Interestingly, the model that consistently emerges as best is the fixed-density model, in which globulars arise from perturbations over a fixed density threshold that is constant everywhere in the universe. Unfortunately, this is one of the two models that is not well justified on physical grounds. Conversely, the model in which there is at least an attempt to incorporate a physical effect—the density-contrast model—is the one that fares worst in almost every test.

In addition to structural properties and dependence on Hubble type, the metallicities of globular clusters provide a further stringent test of cluster models. As already noted, the radial gradient problem in Milky Way clusters is solved by Zinn's isolation of the disk component from the halo component. This stratagem might work for other spirals, but it clearly will not work for Es, which have no disk. So far the only E with a known metallicity gradient is M87 (Strom *et al.* 1981).
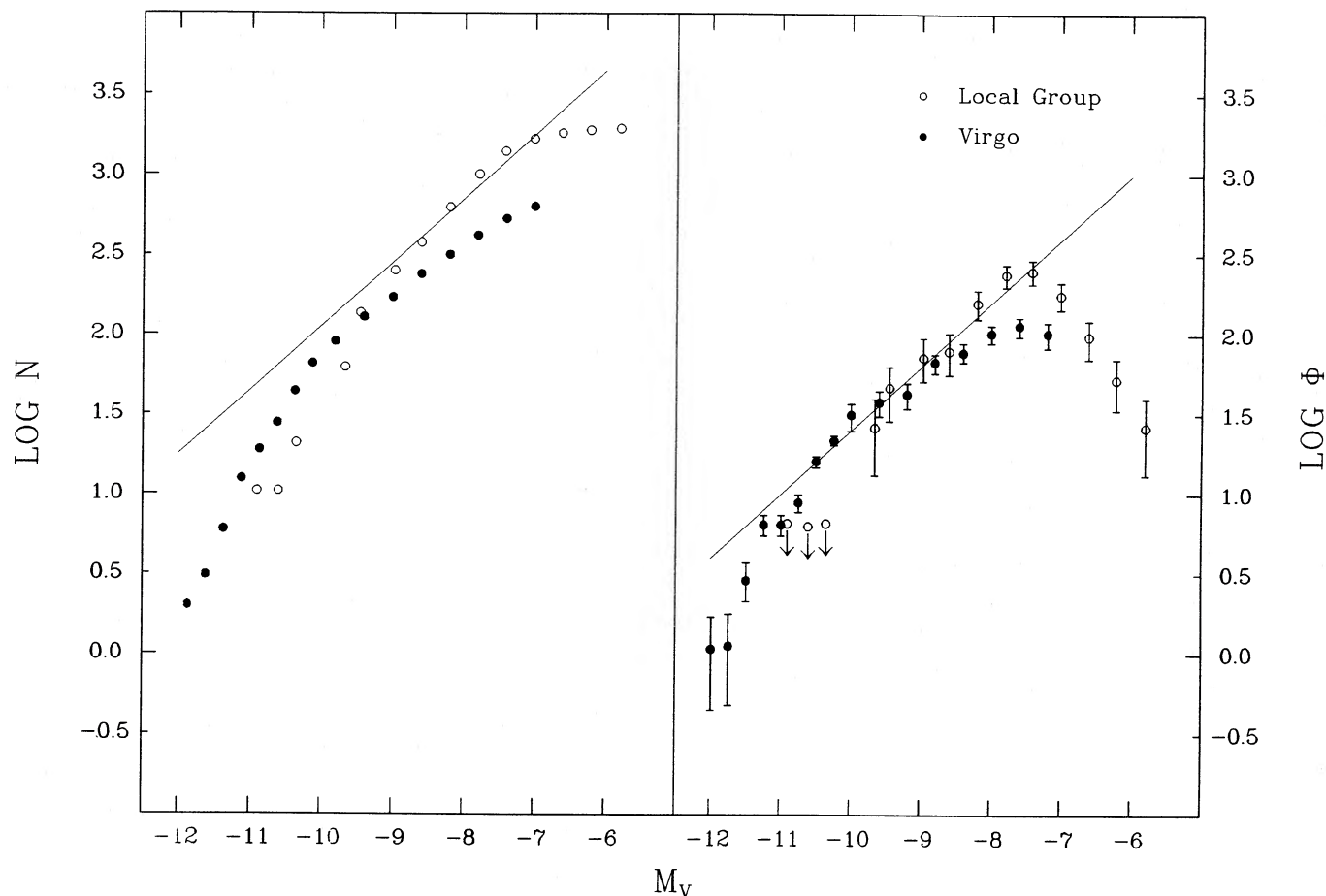
FIG. 5.—The differential and integral luminosity functions of globular clusters in the Local Group (*open circles*) and Virgo Cluster (*dots*). $N(M_V)$ is the total number of globulars brighter than M_V, with Virgo normalized to the Local Group. $\Phi(M_V)$ is the differential function dN/dM_V. The data in this figure were generously communicated by William Harris and represent the most recent update to two figures shown in Harris and Racine (1979). The predicted relations $N(M_V) \approx M^{-1}$ and $\Phi(M_V) \approx M^{-1}$ of eqs. (1) and (2) are shown as the straight lines. The equations fit the data well for $M_V \geq -9$ but depart from them above this level.

However, if globular gradients prove to be a general phenomenon in E's, this would show that at least some of the globulars in ellipticals are not pregalactic.

Leonard Searle (private communication) raises another point. The mean metallicity of M31 globulars is considerably higher than those in the Milky Way, and this is true even if the sample is restricted to clusters with spheroid kinematics. How

this might happen in a purely pregalactic picture is so far unexplained.

This point is an example of a more general problem: what controls the final metal abundance of each cluster in the pregalactic picture, and how does the metallicity *within* each cluster manage to be so uniform? If globulars really are the very first structures in the universe to form, by definition there can be no

TABLE 3

SUMMARY OF MODEL SUCCESSES[a]

Observation	Fixed-Density	Fixed-Probability	Density-Contrast
Globular structural properties vs. Hubble type	*Same in all types*	*Same in all types*	Strongly dependent on type
Cluster mass fraction vs. Hubble type	*Higher in early types*	Same in all types	Lower in early types
Radial distribution of globulars in galaxies relative to dark matter	*More concentrated*	Same	Less Concentrated
Globular luminosity function	*Fair fit*[b]	*Fair fit*[b]	Fair fit (?)[c]

[a] Successes are denoted by italics.
[b] Provided some dynamical friction is invoked to remove brightest clusters.
[c] Prediction less certain than the other two models.

prior generations of stars to preenrich and homogenize the interstellar medium. For this reason, it is hard to avoid returning after all to Peeble's conclusion that the clusters must be self-enriched. To minimize the internal abundance spread then requires a variable IMF such that the first stars were exclusively massive ones that enriched and homogenized the gas. After this initial phase, there must have been a rapid transition to a normal IMF, after which the cluster as we see it today was formed. Adjusting the IMF in this way can minimize the internal abundance spread but still does not answer what controls the final metal abundance of each cluster, or why this varies from cluster to cluster or from galaxy to galaxy.

It might appear tempting to try to merge the pregalactic and secondary theories and thereby capture the best features of both. For example, one might argue that primordial CDM fluctuations act as seeds for the Fall-Rees cooling instability or for clouds in the cloud-cloud collision model. Such models may work well dynamically, but they do not solve the metallicity problem any more convincingly than the purely pregalactic picture. For, unless we want to adopt the self-enriched model with its variable IMF and other questions, we are still left with the need to enrich the ISM homogeneously to high levels on cluster-sized scales. This implies a prior generation of stars, and hence a prior generation of collapsed fluctuations. It is then difficult to continue to identify globular clusters with the seeds of the *first* generation to collapse, which is the essence of the pregalactic picture.

IV. SUMMARY

We have re-examined the Peebles-Dicke hypothesis for pregalactic globular cluster formation in the light of Zinn's discovery of a two-component globular population in the Milky Way. Although the calculations explicitly assume a cold dark matter density fluctuation spectrum, qualitatively the results would apply to any random-phase theory with a flat spectrum in the range 10^6–10^{12} $M_\odot$. Peebles (1984) has previously considered such a picture, but we amend his results slightly by assuming that only high-σ fluctuations of 10^{5-6} $M_\odot$ survive as globular clusters. This assumption seems more intuitive and

also yields smaller, denser structures that agree better with observations.

To match the mass fraction of galaxies in globulars requires that perturbations above roughly 2.8 σ survive as globulars. To match the observed radii and densities of clusters then requires baryonic collapse factors of order 10. Although there is no known mechanism whereby structures can dissipate by such a large factor and still not rotate strongly, the magnitude of the problem is not much worse than for elliptical galaxies. Perhaps a similar mechanism to suppress angular momentum operates in both cases.

An attempt is made to compare the theory with the observed properties of globular clusters. The results are found to depend sensitively on the precise survival scheme for globulars that is assumed. The scheme that seems to work best is the assumption that all fluctuations above a fixed threshold σ that is globally defined over the whole universe survive as globulars. This means that the absolute value of the density threshold decreases somewhat with cluster mass but is independent of local environment. For a density threshold level of roughly 2.8 σ, adequate fits are achieved to cluster radii and densities, the mass fraction of globulars versus Hubble type, the radial density profiles of globulars within galaxies, and the globular luminosity function.

On the negative side, this particular rule for globular survival seems rather arbitrary and lacks a convincing physical justification. Another major question is globular cluster metallicities: how can clusters be so homogeneous internally yet show such large scatter from cluster to cluster and from galaxy to galaxy? It is tempting to try to merge the pregalactic and secondary scenarios to solve these problems, but exactly how to do this and preserve the identification with true primordial density fluctuations is not clear.

We conclude that the pregalactic model as applied to Zinn's pure halo population achieves some tantalizing successes but still presents some important, unanswered questions.

REFERENCES

Bardeen, J. M., Bond, J. R., Kaiser, N., and Szalay, A. S. 1986, *Ap. J.*, **304**, 15.
Blumenthal, G. R., Faber, S. M., Flores, R., and Primack, J. R. 1986, *Ap. J.*, **301**, 27.
Blumenthal, G. R., Faber, S. M., Primack, J. R., and Rees, M. J. 1984, *Nature* **311**, 517 (BFPR).
Burstein, D. 1987, in *Nearly Normal Galaxies: From the Planck Time to the Present*, ed. S. M. Faber (New York: Springer Verlag), p. 47.
Burstein, D., Faber, S. M., Gaskell, C. M., and Krumm, N. 1984, *Ap. J.*, **287**, 586.
Christian, C. R., Heasley, J. W., and Janes, K. A. 1985, *Ap. J.*, **299**, 683.
Christian, C. R., and Schommer, R. A. 1983, *Ap. J.*, **275**, 92.
David, M. C., and Peebles, P. J. E. 1983, *Ap. J.* **267**, 465.
Fall, S. M., and Rees, M. J. 1985, *Ap. J.*, **298**, 18.
———. 1986, in *Stellar Populations*, ed. C. Norman, A. Renzini, and M. Tosi (Cambridge: Cambridge University Press), in press.
Forte, J. C., Strom, S. E., and Strom, K. M. 1981, *Ap. J. (Letters)*, **245**, L9.
Freeman, K. C. 1980, in *IAU Symposium 85, Star Clusters*, ed. J. D. Hesser (Dordrecht: Reidel), p. 317.
Gunn, J. E. 1980, in *Globular Clusters*, ed. D. Hanes and B. Madore (Cambridge: Cambridge Univesity Press), p. 301.
Gunn, J. E., and Griffin, R. F. 1979, *A.J.*, **84**, 752.
Harris, W. E. 1986, *A. J.*, **91**, 822.
———. 1987, *Pub. A.S.P.*, in press.

Harris, W. E., and Racine, R. 1979, *Ann. Rev. Astr. Ap.*, **17**, 241.
Harris, W. E., and van den Bergh, S. 1982, *A.J.*, **86**, 1627.
Illingworth, G. 1976, *Ap. J.*, **204**, 73.
Kraft, R. P. 1979, *Ann. Rev. Astr. Ap.*, **17**, 309.
Lauer, T., and Kormendy, J. 1987, in preparation.
Peacock, J. A., and Heavens, A. F. 1986, preprint.
Peebles, P. J. E., 1980, *The Large-Scale Structure of the Universe* (Princeton: Princeton University Press).
———. 1984, *Ap. J.*, **277**, 470.
Peebles, P. J. E., and Dicke, R. H. 1968, *Ap. J.*, **154**, 891.
Peterson, C., and King, I. R. 1975, *A.J.*, **80**, 427.
Primack, J. R., and Blumenthal, G. R. 1985, in *Clusters and Groups of Galaxies*, ed. F. Mardirossian, G. Guercin, and M. Mezzetti (Dordrecht: Reidel), p. 435.
Quinn, P. J., and Goodman, J. 1986, *Ap. J.*, **309**, 472.
Strom, S. E., Forte, J. C., Harris, W. E., Strom, K. M., Wells, D. C., and Smith, M. G. 1981, *Ap. J.*, **245**, 416.
Tremaine, S. D. 1976, *Ap. J.*, **203**, 345.
van den Bergh, S., and Harris, W. E., 1982, *A.J.*, **87**, 494.
Zinn, R. W. 1978, *Ap. J.*, **225**, 790.
———. 1985, *Ap. J.*, **293**, 424.

GEORGE R. BLUMENTHAL, S. M. FABER, and EDWARD I. ROSENBLATT: Board of Studies in Astronomy and Astrophysics, Lick Observatory, University of California, Santa Cruz, CA   95064